Park et al.
Journal of Analytical Science and Technology (2023) 14:17
https://doi.org/10.1186/s40543-023-00380-7

Journal of Analytical Science and Technology

RESEARCH ARTICLE
Open Access

Benefits of high-dielectric pad for neuroimaging study in 7-Tesla MRI

Shin-Eui Park[1,2], Yeong-Jae Jeon[3] and Hyeon-Man Baek[2,3*]

Abstract

This study aimed to evaluate whether the use of a high-dielectric pad is effective in increasing transmit and receive sensitivity in areas of low signal intensity in the human brain at high magnetic fields and assess its usefulness in neuroimaging studies. The novelty of this study lies in the first reported use of diffusion tensor imaging (DTI) results to evaluate the effect of the pad on neuroimaging. Six volunteers underwent MR scanning using a 7 T MR system. T1-weighted images (T1w) and diffusion-weighted images (DWI) were acquired to demonstrate the benefits of a high-dielectric pad made of barium titanate ($BaTiO_3$). For all imaging experiments, two datasets were acquired per person, one with and one without a high-dielectric pad. Enhancement of signal sensitivity in neuroimaging has been analyzed by DTI study. Higher signal intensities and spatial contrast were demonstrated in the in T1w images acquired using high-dielectric pad than in those acquired without high-dielectric pad. Especially in DTI studies, increased quantitative anisotropy (QA) signals were observed in the corticospinal tract (CST), frontopontine tract (FPT), splenium of corpus callosum (SCC), fornix (FX), inferior fronto-occipital fasciculus (IFOF), cerebellum (CB), middle cerebellar peduncle (MCP), and body of corpus callosum (BCC) (FDR < 0.05). The signal differences accounted for an overall 20% increase. A high-dielectric pad is effective in enhancing signal intensity in human brain images acquired using 7 T MRI. Our results show that the use of such pad can increase the spatial resolution, tissue contrast, and signal intensity in neuroimaging studies. These findings suggest that high-dielectric pads may provide a relatively simple and low-cost method for spatiotemporal brain imaging studies.

Keywords High-dielectric pad, Ultra-high field MRI, Diffusion tensor imaging, High signal intensity, High tissue contrast

Background

Theoretically, ultra-high field magnetic resonance imaging (MRI) ($\geq$7 T) has a higher signal-to-noise ratio (SNR), which leads to higher spatiotemporal resolution and enhanced tissue contrast, compared with lower-field MRI ($\leq$3 T) (Vaughan et al. 2001). However, ultra-high field imaging faces technical challenges due to radiofrequency (RF) inhomogeneity, increased tissue heating, and reduced wavelength of the RF field (B1). To compensate for B1 interference with the human body, RF shimming is commonly used; it is a technique that uses a transmit array (active shimming) and high-dielectric material (passive shimming) (Steensma et al. 2019). Compared to the active shimming required for advanced coil designs and additional hardware, passive shimming, such as the use of high-dielectric pads placed between the coils and the human body, is a more cost effective and straightforward approach to significantly improve image quality. The high-dielectric pad is composed of high-permittivity materials (e.g., barium titanate [$BaTiO_3$] and calcium titanate [$CaTiO_3$]), which are effective in altering the spatial distribution of electromagnetic fields and enlarging

*Correspondence:
Hyeon-Man Baek
hmbaek98@gachon.ac.kr
[1] Department of Radiology, Weill Cornell Medicine, New York, NY, USA
[2] Lee Gil Ya Cancer and Diabetes Institute, Gachon University, # 155 Gaetbeol-ro Yeonsu-gu, Incheon 21999, Korea
[3] Department of Health Science and Technology, GAIHST, Gachon University, Incheon 21936, Korea

the shortened wavelength of B1 for high-field MRI applications of the brain or body (Teeuwisse et al. 2012a). This high-dielectric pad could be useful for neuroimaging studies targeting subcortical structures in the brain using ultra-high field MRI. To date, most previous studies have demonstrated the effectiveness of high-dielectric pads in neuroimaging by comparing simulations and/or images, such as B0, B1, specific absorption rate (SAR), echo planar imaging (EPI), and T1 and T2 images (O'Reilly et al. 2016; Teeuwisse et al. 2012b; Van Gemert et al. 2019). Although these methods are useful for estimating image quality, data post-processing are needed for a more accurate and specific neuroimaging evaluation.

In this study, we evaluated the effect of a high-dielectric pad in a neuroimaging study using a 7 T MRI scanner, and the pad was placed around the subject's inner birdcage head coil. T1-weighted images (T1w) and diffusion weighted images (DWI) were acquired to evaluate feasibility of high-dielectric pad to enhance anatomical and neuronal imaging.

Methods

High-dielectric pad

Two pads of dimensions 440 (width) × 220 (length) × 2 (height) mm^3 were formed. Ba-TiO_3 (Alfa Aesar, Ward Hill, MA) mixed in deuterated water (35%) was prepared and heat-sealed within a polypropylene pad after removing as much entrapped air as possible. This high-dielectric pad was placed to cover the subjects' heads (Fig. 1). The permittivity of the high-dielectric pad was approximately 215. Aqueous suspension of barium titanate (εr ~ 2000) in deionized water (εr ~ 80) was prepared at room temperature. The barium titanate was mixed with distilled, deionized water in volume/volume ratios to 40%. Complex permittivity measurements were performed using a dielectric assessment kit (DAK-12, SPEAG, Zurich, Switzerland). The relative permittivity with a saturated suspension of 35% (v/v) is approximately 215.

Data acquisition

For all imaging experiments, two datasets were acquired per person, one with and one without a high-dielectric pad. Six volunteers (age range = 25–52 years, mean age = 38.17 ± 11.89 years, male/female = 5/1) were included in the study, with approval from the local medical ethics committee.

All subjects underwent MRI using a 7 T MR system (Magnetom Terra, Siemens Healthcare, Erlangen, Germany) with a 32-channel phased-array head coil (Nova Medical, Wilmington, MA, USA). Three-dimensional (3D) anatomical brain scans were acquired using magnetization prepared rapid acquisition gradient echo (MP-RAGE) sequence-induced T1w images with the following settings: repetition time (TR) = 4500 ms, echo time (TE) = 1.48 ms, flip angle (FA) = 6°, slice thickness = 0.8 mm, in-plane resolution = 0.8 × 0.8 mm^2, matrix size = 304 × 304, number of slices = 192, total scan time = 8 min 8 s. Diffusion weighted images (DWI) were acquired using a multiband spin-echo EPI sequence with the following setting: TR/TE = 6800/72 ms, slice thickness = 1.2 mm, in-plane resolution = 1.2 × 1.2 mm^2, matrix size = 180 × 180, number of slices = 109, b-value = 2500 s/mm^2, 64 diffusion weighting directions, total scan time = 17 min 56 s.

DTI-based assessment of magnetic susceptibility effects

Group connectometry analysis was performed using DSI-studio software (https://dsi-studio.labsolver.org) to study the effect of the high-dielectric pad. Diffusion data were reconstructed in the MNI space using q-space diffeomorphic reconstruction (QSDR) (Yeh et al. 2016) to obtain the spin distribution function (SDF) (with sample length ratio = 1.25), which was sampled by local fiber directions from the common atlas to estimate the local connectome. A t-score threshold of 2.5 was assigned and tracked using a deterministic fiber tracking algorithm (Yeh et al. 2016) to obtain correlational tractography. The seeding region was placed throughout the brain. The tracks

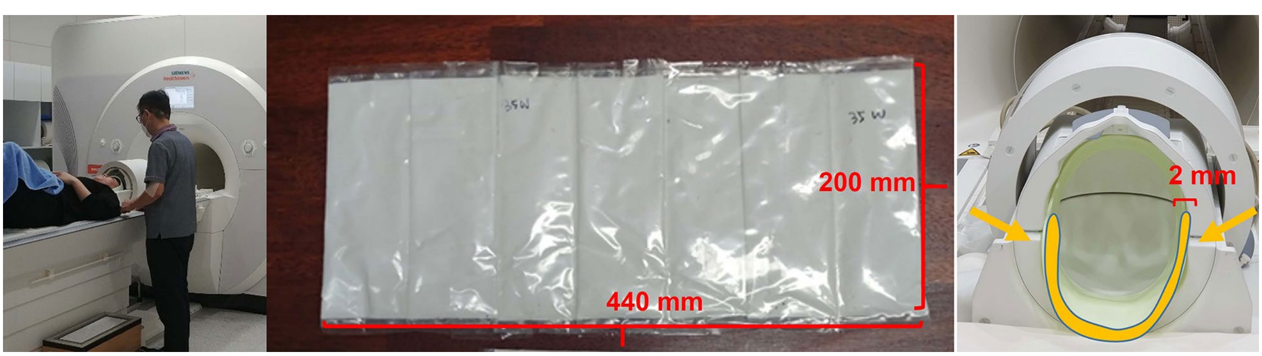

Fig. 1 Photograph of experimental method, shape and position of high-dielectric pad (orange arrow)

were filtered using topology informed pruning (Yeh et al. 2016) with four iterations. A length threshold of 20 voxels was used to select tracks. To estimate the false discovery rate (FDR), 4000 randomized permutations were applied to the group label to obtain the null distribution of track length. The paired t test was used to analyze differences between with and without high-dielectric pad. The fiber track increase rate was calculated as follows:

$$\frac{\text{Observed fiber tracks with high} - \text{dielectric pad minus Observed fiber tracks without pad}}{\text{Total fiber tracks (in each region)}} \times 100(\%)$$

Results

Anatomical image results

Figure 2 shows three representative slices of T1w images with and without a high-dielectric pad. There was no apparent signal dropout and distortion in images with the addition of the high-dielectric pad. The mean signal intensities between with and without pad were 82.23 ± 109.13 (maximum intensity: 1168) and 82.15 ± 110.14 (maximum intensity: 1321), respectively. It seems that the rough signal due to the B1 field inhomogeneity appears to have been compensated for by passive shimming.

DTI image results

Compared to the images acquired without high-dielectric pad, those acquired with high-dielectric pad showed a significantly higher quantitative anisotropy (QA) signal in the corticospinal tract (CST), frontopontine tract (FPT), splenium of the corpus callosum (SCC), fornix (FX), inferior fronto-occipital fasciculus (IFOF), cerebellum (CB), middle cerebellar peduncle (MCP), and body of the corpus callosum (BCC) ($p < 0.003$). Out of them, the FX ($p < 0.035$) and IFOF ($p < 0.044$) regions were significantly observed in each sub-region (false discovery rate; FDR < 0.05) (Figs. 3, 4, 5; Table 1). The fiber track increase rate differences accounted for an overall 20% increase (fiber track increase rate observed in whole brain). In the case of the sub-regions, the fiber track increase rate differences were observed as follows: 12% increase in CST, 17% increase in FPT, 27% increase in FX, 20% increase in IFOF, 8% increase in CB, 14% increase in MCP, and 4% increase in BCC. Figure 6 shows increased number of fiber tracks by using high-dielectric pad.

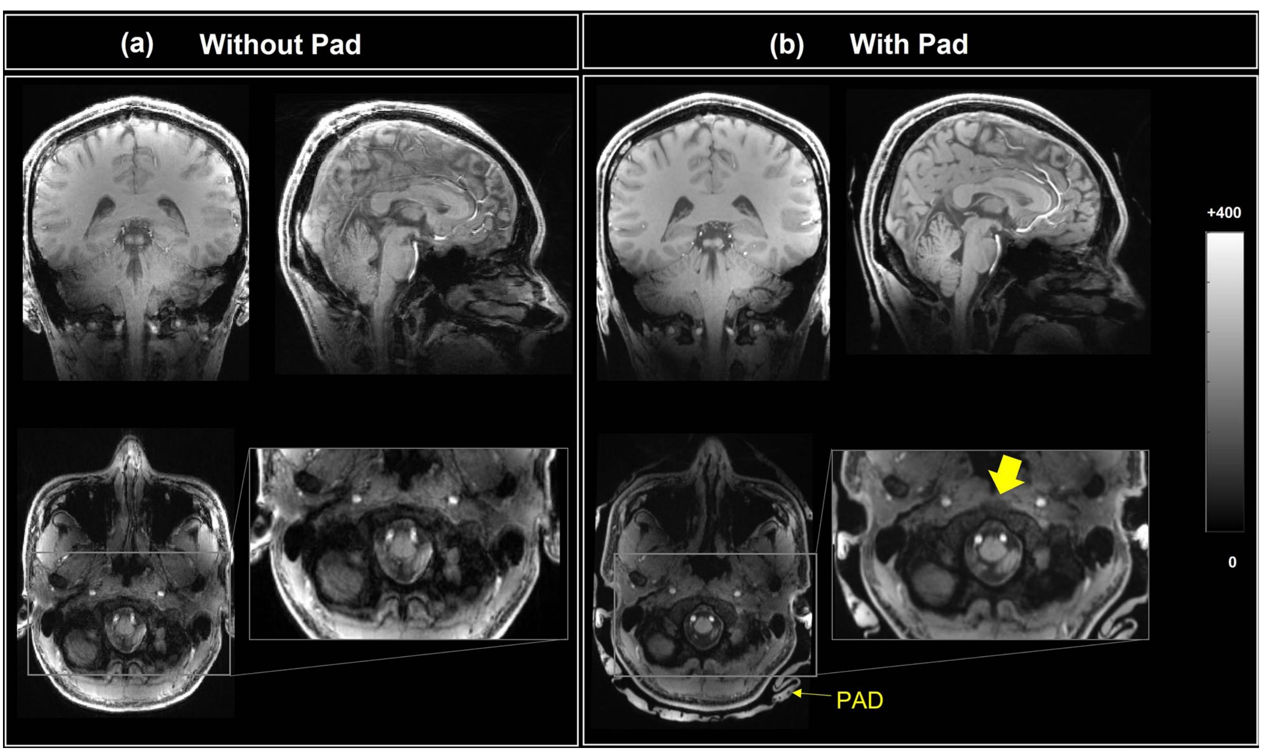

Fig. 2 Images were acquired to investigate any effects of the high-dielectric pad in T1-weighted images using 7 T MRI. **a** and **b** corresponding images acquired with and without high-dielectric pads, respectively. Increased tissue contrast and signal intensity are observed in images with pad (**b**) compared to those without pad (**a**). The yellow arrow indicates the representative area of enhanced tissue contrast

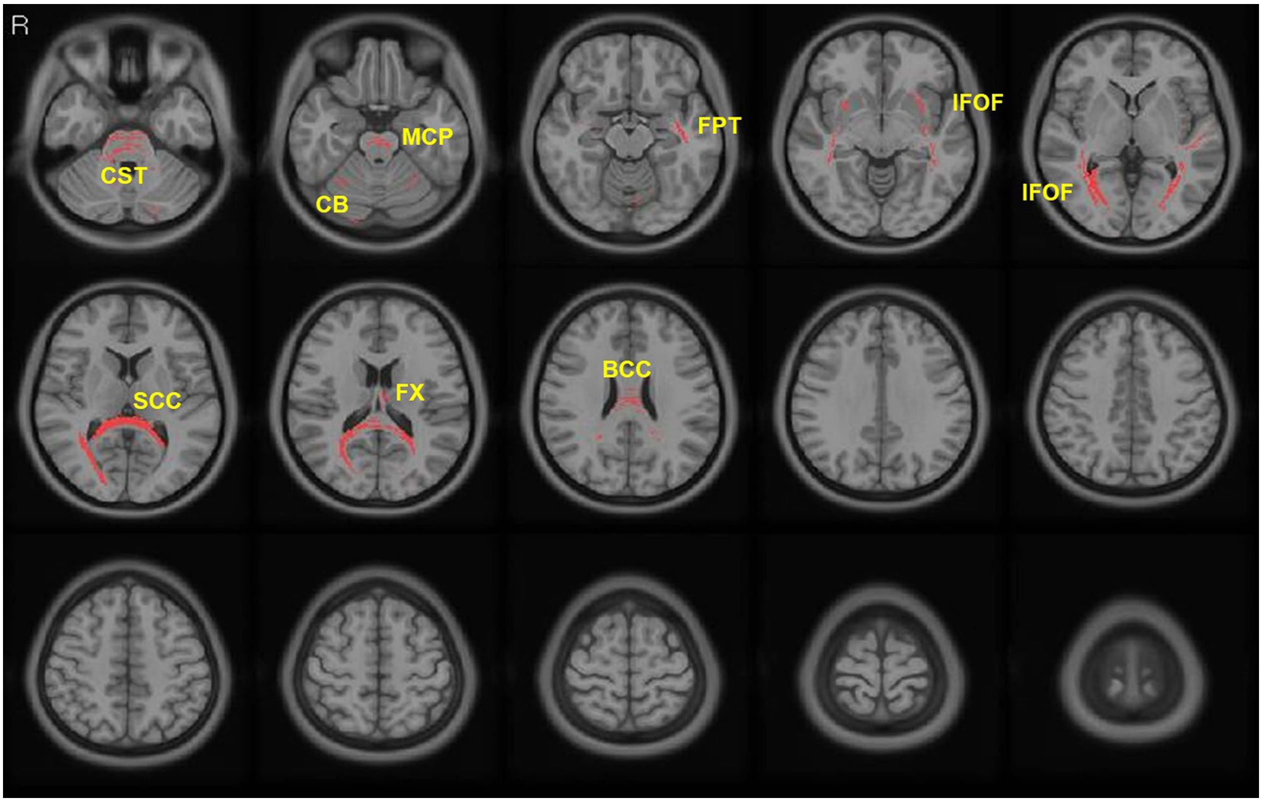

Fig. 3 Axial planes showing quantitative anisotropy (QA) signal enhancement in the brain using high-dielectric pad. *CST* Corticospinal tract; *MCP* Middle cerebellar peduncle; *CB* Cerebellum; *FPT* Frontopontine tract; *IFOF* Inferior fronto-occipital fasciculus; *SCC* Splenium of corpus callosum; *FX* Fornix; *BCC* Body of corpus callosum

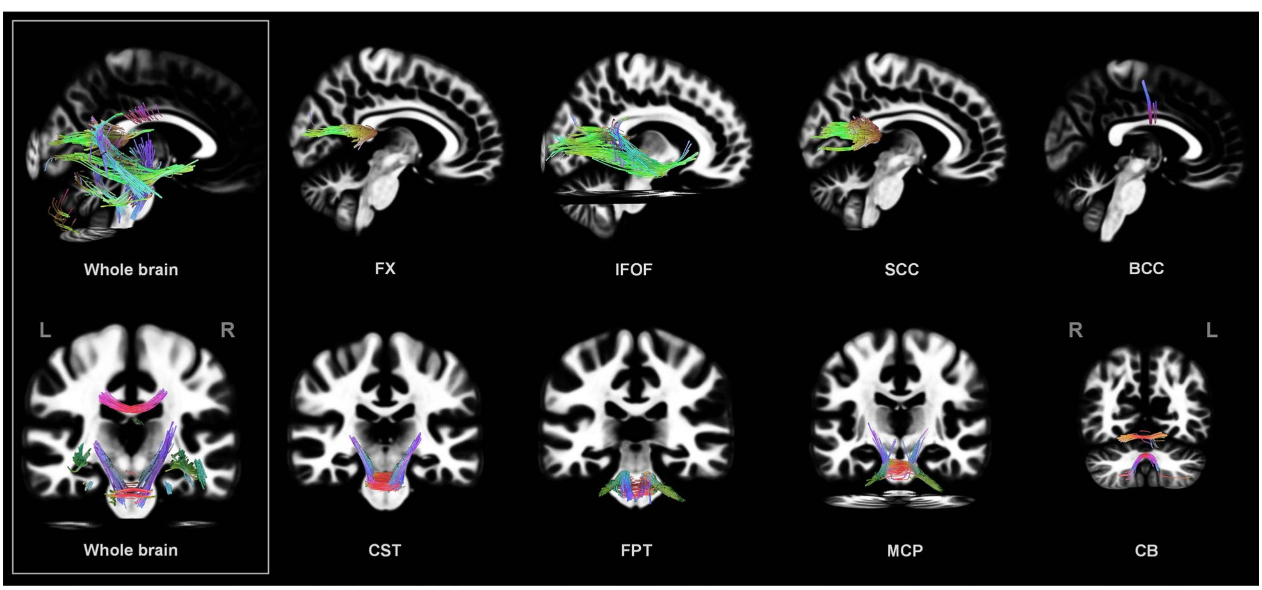

Fig. 4 Three-dimension tractography showing the signal enhancement area using high-dielectric pad. The different colors represent different directions of the neuronal fibers. *FX* Fornix; *IFOF* Inferior fronto-occipital fasciculus; *SCC* Splenium of corpus callosum; *BCC* Body of corpus callosum; *CST* Corticospinal tract; *FPT* Frontopontine tract; *MCP* Middle cerebellar peduncle; *CB* Cerebellum

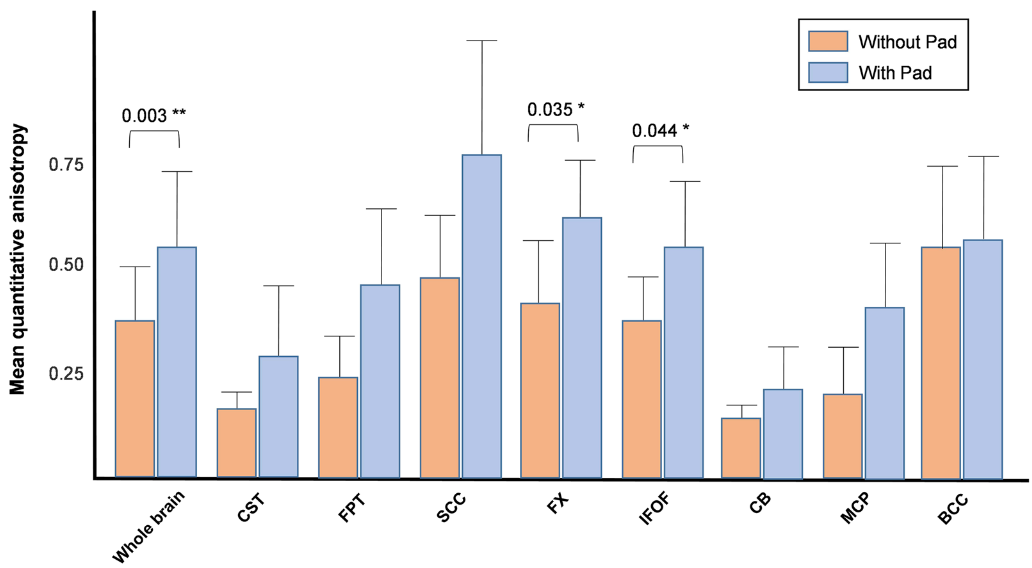

Fig. 5 A bar graph showing the comparison between mean quantitative anisotropy (QA) values with and without the use of high-dielectric pad. Asterisk denotes significant difference with increased QA value when compared to that without pad. *CST* Corticospinal tract; *FPT* Frontopontine tract; *SCC* Splenium of corpus callosum; *FX* Fornix; *IFOF* Inferior fronto-occipital fasciculus; *CB* Cerebellum; *MCP* Middle cerebellar peduncle; *BCC* Body of corpus callosum

Table 1 Brain areas showing significantly increased quantitative anisotropy (QA) values with high-dielectric pad compared to those without it

Regions	Pad		*p*-Value	No. fiber tracks
	Without	With		
Whole brain	0.36 ± 0.19	0.56 ± 0.26	0.003**	6690
Corticospinal tract (CST)	0.15 ± 0.07	0.27 ± 0.21	0.150	2997
Frontopontine tract (FPT)	0.23 ± 0.16	0.40 ± 0.25	0.184	1863
Splenium of the corpus callosum (SCC)	0.49 ± 0.26	0.76 ± 0.32	0.088	815
Fornix (FX)	0.37 ± 0.20	0.64 ± 0.20	0.035*	517
Inferior fronto-occipital fasciculus (IFOF)	0.35 ± 0.18	0.55 ± 0.25	0.044*	240
Cerebellum (CB)	0.14 ± 0.06	0.22 ± 0.13	0.111	121
Middle cerebellar peduncle (MCP)	0.19 ± 0.11	0.33 ± 0.24	0.170	105
Body of the corpus callosum (BCC)	0.52 ± 0.25	0.56 ± 0.25	0.656	32

p-Values of Paired-samples *t* test

*Statistically significant with *p*-value < 0.05

**Statistically significant with *p*-value < 0.01

Discussion

In this study, we applied high-dielectric pads around the human brain using 7 T MRI system equipment that showed enhanced spatial resolution and tissue contrast in anatomical images, and increased signal intensity in DTI results. Among DTI values, QA was used. Neuroimaging studies commonly use fractional anisotropy (FA) values rather than QA values in DTI study, however there are differences between them. FA is defined for each voxel and associated with axonal integrity. On the other hand, QA is defined for each fiber orientation and associated with axonal density (Yeh et al. 2019). Both QA and FA values decrease when there is axonal loss in the brain. However, although QA and FA have similar meanings, we wanted to focus on axonal density rather than axonal integrity. The T1w images in Fig. 2 show improved image SNR and tissue contrast without magnetic susceptibility induced artifacts when acquired using the high-dielectric pad. It seems that high permittivity materials increase the strength of the transmit (B1 +) and receive (B1 −) magnetic fields in areas that have intrinsically low sensitivity owing to both

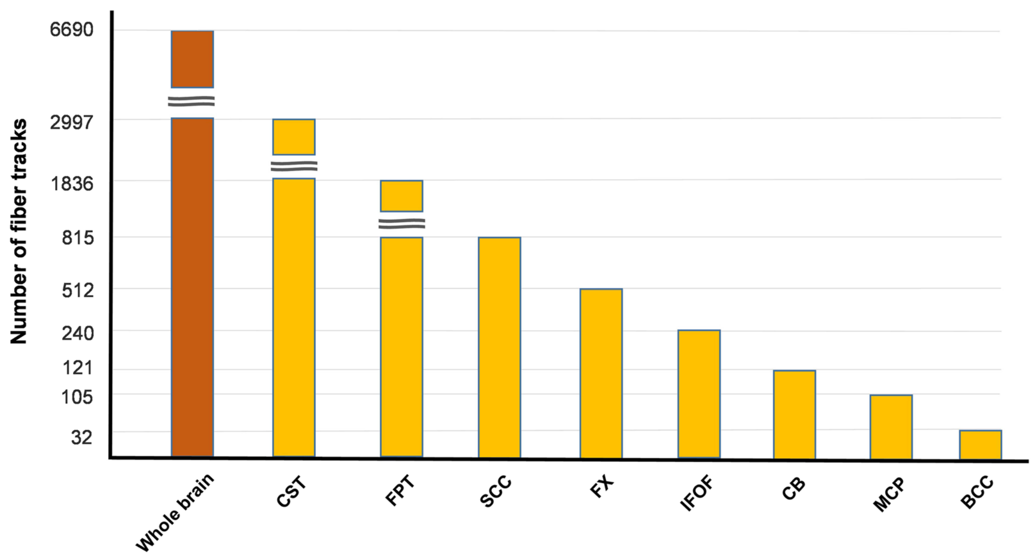

Fig. 6 Increased number of neuronal fiber tracks with high-dielectric pad compared to without. *CST* Corticospinal tract; *FPT* Frontopontine tract; *SCC* Splenium of corpus callosum; *FX* Fornix; *IFOF* Inferior fronto-occipital fasciculus; *CB* Cerebellum; *MCP* Middle cerebellar peduncle; *BCC* Body of corpus callosum

geometry and high operating frequency (Haines et al. 2010; Snaar et al. 2011; Yang et al. 2006). Our results are consistent with those reported by a previous study (Teeuwisse et al. 2012a), suggesting that high-dielectric pads have enhanced SNR with no detrimental effect of magnetic susceptibility on the brain image at 7 T MRI. On the other hand, the brain image using high-dielectric pad (Fig. 2b) was blurrier than image of without pad (Fig. 2a). It seems effects of low-pass filtering. Low-pass filters are commonly used in MRI to reduce the impact of high-frequency noise in the imaging data. By using a high-dielectric material, the filter effect can be greatly enhanced, allowing for the effective reduction in high-frequency noise and the improvement of image quality. Also, the dielectric constant of a material, combined with its physical properties, can greatly impact the performance of the low-pass filter and the overall quality of the MRI images produced. However, additional simulation and experimental results are required to demonstrate the spectral distribution in the electromagnetic field in further studies. One of the challenges of EPI are artifacts which associated with signal loss and imaging blurring leading to non-diagnostic quality derived from B1 field inhomogeneity (Afacan et al. 2019). In this case, high-resolution EPI images come to overcome, providing high-quality, high-resolution images (Afacan et al. 2019). However, this approach has practical limitations such as time consumption and/or SAR increase. These issues pose challenges to most of neuroimaging studies. Here, we propose possibility for the solution with high-dielectric pad.

The DTI results shown in Figs. 3 and 4 show higher signal intensity in the high-dielectric pad than in the control without pad, especially in subcortical brain regions. The overall signal difference increases by 20%. The Fx, which is a part of the limbic system, carries afferent fibers to the hippocampus from the diencephalon and basal forebrain. This structural process is most closely associated with memory function (Kim et al. 2013). Previous studies have reported that fractional anisotropy (FA) in the Fx decreases with advanced age, correlates with age-related memory impairments (Kim et al. 2013), and is relatively decreased in mild cognitive impairment and Alzheimer's disease symptoms (Lee et al. 2019).

As a long associative bundle, the IFOF passes through the temporal lobe and insula, connecting the occipital cortex, temporo-basal areas, and superior parietal lobe to the frontal lobe (Bae et al. 2021). The IFOF has also been reported to play an important role in reading, attention, and visual processing (Benear et al. 2020; Douet and Chang 2015).

To date, there have been many attempts to define neural mechanisms and/or diagnostic biomarkers in clinical application studies, targeting subcortical regions (Schmahmann and Pandya 2007; Martino et al. 2010; Catani. 2008). Conventional MRI (1.5-3 T MRI) is reliable for detecting complete segmentation in the whole brain, but it is difficult to identify detailed subcortical regions due to poor contrast and low intensity signals. In addition, advanced coil designs and additional hardware are required to compensate for the magnetic inhomogeneity, in ultrahigh field MRI. Our results suggest that using a high-dielectric pad may provide a simple and low-cost method for more advanced neuroimaging studies.

This study has several limitations. First, the sample size was relatively small, consisting of only six volunteers. Second, there are no B1 and B0 simulations and imaging analyses for magnet and RF field homogeneity. Correlation analysis between B1 improvement and increased QA value would be a strong proof of the feasibility of high-dielectric Pad. Third, there are no SAR simulation or imaging analyses to demonstrate reduced tissue heating. Optimized experimentation is needed to obtain better results in future studies, considering these limitations.

Conclusions

Our results showed increased QA values in CST, MCP, CB, FPT, IFOF, SCC, FX and BCC with high-dielectric pad in DTI study in ultra-high field MRI. These brain regions were known as key regions in many neuroimaging studies. These signal increases are presumably associated with regional B1 field homogeneity although quantitative results were not obtained. This study suggests feasibility of high-dielectric pad to enhanced human brain imaging and neuroimaging study in ultra-high field MRI. In particular, it will be useful to get an enhanced data quality at deep brain regions which are vulnerable to contamination by magnet field inhomogeneity in ultra-high field MRI. Also, our study would be the basis for further specialized studies using quantitative and qualitative approach.

Abbreviations

MRI	Magnetic resonance imaging
SNR	Signal-to-noise ratio
RF	Radiofrequency
B1	RF field
SAR	Specific absorption rate
EPI	Echo planar imaging
T1w	T1-weighted images
DWI	Diffusion weighted images
DTI	Diffusion tensor imaging
$BaTiO_3$	Barium titanate
3D	Three-dimensional
MP-RAGE	Magnetization prepared rapid acquisition gradient echo
TR	Repetition time
TE	Echo time
FA	Flip angle
AC	Anterior commissure
PC	Posterior commissure
FDR	False discovery rate
QSDR	Q-space diffeomorphic reconstruction
SDF	Spin distribution function
QA	Quantitative anisotropy
CST	Corticospinal tract
FPT	Frontopontine tract
SCC	Splenium of corpus callosum
FX	Fornix
IFOF	Inferior fronto-occipital fasciculus
CB	Cerebellum
MCP	Middle cerebellar peduncle
BCC	Body of corpus callosum

Acknowledgements
Not applicable.

Author contributions
Y-JJ and H-MB designed the studies. Y-JJ conducted a high-dielectric pad, MRI experiment, and acquired data. S-EP and Y-JJ contributed to the analysis and interpretation of the data. S-EP wrote the first draft of the manuscript. HMB has approved the final manuscript and completed manuscript. All the authors agree with the content of the manuscript.

Funding
This research supported by Basic Science Research Capacity Enhancement Project through Korea Basic Science Institute (National research Facilities and Equipment Center) grant funded by the Ministry of Education (Grant no. 2021R1A6C101A432), and Bio & Medical Technology Development Program of the National Research Foundation funded by the Korea government (MSIT) (2020M3A9E4104384).

Availability of data and materials
No supporting data are included.

Declarations

Competing interests
No supporting data are included.

Received: 21 November 2022 Accepted: 19 February 2023
Published online: 06 March 2023

References

Afacan O, et al. Fetal echoplanar imaging: promises and challenges. Top Magn Reson Imaging. 2019;28(5):245–54.
Bae Y-J, et al. Imaging the substantia nigra in Parkinson disease and other parkinsonian syndromes. Radiology. 2021;300(2):260–78.
Benear SL, Ngo CT, Olson IR. Dissecting the fornix in basic memory processes and neuropsychiatric disease: a review. Brain Connect. 2020;10(7):331–54.
Catani M, Thiebaut de Schotten M. A diffusion tensor imaging tractography atlas for virtual in vivo dissections. Cortex. 2008;44(8):1105–32.
Douet V, Chang L. Fornix as an imaging marker for episodic memory deficits in healthy aging and in various neurological disorders. Front Aging Neurosci. 2015;6:343.
Haines K, Smith NB, Webb AG. New high dielectric constant materials for tailoring the B1+ distribution at high magnetic fields. J Magn Reson. 2010;203(2):323–7.
Kim J-H, Song S-K. Diffusion tensor imaging of the mouse brainstem and cervical spinal cord. Nat Protoc. 2013;8(2):409–17.
Lee Y-J, et al. Atrophic changes and diffusion abnormalities of affected trigeminal nerves in trigeminal neuralgia using 7-T MRI. Stereotact Funct Neurosurg. 2019;97(3):169–75.
Martino J, et al. Anatomic dissection of the inferior fronto-occipital fasciculus revisited in the lights of brain stimulation data. Cortex. 2010;46(5):691–9.
O'Reilly TPA, Webb AG, Brink WM. Practical improvements in the design of high permittivity pads for dielectric shimming in neuroimaging at 7 T. J Magn Reson. 2016;270:108–14.
Schmahmann JD, Pandya DN. The complex history of the fronto-occipital fasciculus. J Hist Neurosci. 2007;16(4):362–77.
Snaar JE, et al. Improvements in high-field localized MRS of the medial temporal lobe in humans using new deformable high-dielectric materials. NMR Biomed. 2011;24(7):873–9.
Steensma BR, et al. Comparing signal-to-noise ratio for prostate imaging at 7T and 3T. J Magn Reson Imaging. 2019;49(5):1446–55.
Teeuwisse WM, Brink WM, Webb AG. Quantitative assessment of the effects of high-permittivity pads in 7 Tesla MRI of the brain. Magn Reson Med. 2012a;67(5):1285–93.

Teeuwisse WM, et al. Simulations of high permittivity materials for 7 T neuroimaging and evaluation of a new barium titanate-based dielectric. Magn Reson Med. 2012b;67(4):912–8.
van Gemert J, et al. High-permittivity pad design tool for 7T neuroimaging and 3T body imaging. Magn Reson Med. 2019;81(5):3370–8.
Vaughan JT, et al. 7T vs. 4T: RF power, homogeneity, and signal-to-noise comparison in head images. Magn Reson Med. 2001;46(1):24–30.
Yang QX, et al. Manipulation of image intensity distribution at 7.0 T: passive RF shimming and focusing with dielectric materials. J Magn Reson Imag. 2006;24(1):197–202.
Yeh FC, Badre D, Verstynen T. Connectometry: A statistical approach harnessing the analytical potential of the local connectome. Neuroimage. 2016;125:162–71.
Yeh FC, et al. Differential tractography as a track-based biomarker for neuronal injury. Neuroimage. 2019;202:116131.

Publisher's Note